where

$$A_{12}=\epsilon[(1-\beta)-i\gamma]D,$$
$$A_{23}=\epsilon[-\beta-i\gamma]D,$$
$$B_{13}=\epsilon^3[(1-2\beta)-i\gamma]^{-1}D, \quad (3)$$
$$D=\{[(1-\beta)-i\gamma][-\beta-i\gamma]-\epsilon^2[(1-2\beta)-2i\gamma]/[(1-2\beta)-i\gamma]\}^{-1}, \quad (4)$$

$$\alpha=\epsilon/\gamma,$$
$$\beta=(\omega-\omega_{23})/\delta\omega,$$
$$\gamma=1/(\tau\delta\omega),$$
$$\epsilon=(\gamma H_1)/(2\delta\omega),$$
$$\delta\omega=\omega_{12}-\omega_{23}. \quad (5)$$

PHYSICAL REVIEW VOLUME 106, NUMBER 3 MAY 1, 1957

# Precision Measurement of X-Ray Fine Structure; Effects of Nuclear Size and Quantum Electrodynamics*†

ROBERT L. SHACKLETT‡ AND JESSE W. M. DUMOND
*California Institute of Technology, Pasadena, California*

(Received January 21, 1957)

Schawlow and Townes have made a theoretical calculation of the perturbing effect of the finite size of the nucleus on the $L_{II}$–$L_{III}$ x-ray doublet splitting in heavy elements. Combined with approximate calculations by Christy and Keller of the unperturbed splitting for the case of a point nucleus, comparison of this theory with such experimental values of the splitting as were then available led to an anomalously large value of nuclear radius, $R=r_0A^{\frac{1}{3}}$ with $r_0=2.1\times10^{-13}$ cm. Schawlow and Townes offered the suggestion to account for this that quantum electrodynamic effects probably modify the fine structure in much the same way as an oversize nucleus. The present investigation was undertaken to improve on the precision of the x-ray measurements yielding the $L_{II}$–$L_{III}$ fine structure splitting and to incorporate into a new comparison between theory and experiment the recent vacuum polarization correction of Wichmann and Kroll. The measurements of the $L_{II}$–$L_{III}$ splitting for W, Pt, Bi, Th, U, and Pu are based on two-crystal spectrometer determinations of the Bragg angles of the $L\alpha_2$ and $L\beta_1$ x-ray lines of these elements. Techniques of measurement and corrections for vertical divergence and crystal diffraction pattern asymmetry leading to a relative precision (relative standard deviation) in the splitting of about 50 parts per million are described. A comparison is made with the data used by Schawlow and Townes, and a discrepancy is found in several earlier wavelength values which may account partly for the large value of $r_0$ obtained by them. A comparison of the theoretical to the present experimental values of the splitting, assuming no quantum electrodynamic effects, yields a value of $r_0=1.08\times10^{-13}$ cm. When corrections are made for vacuum polarization and a nuclear radius of $r_0=1.2\times10^{-13}$ cm, a comparison with experiment shows that a discrepancy remains which is then used to evaluate an empirical correction term. The sign, magnitude, and $Z$ dependence of this term suggest that the remaining discrepancy might arise principally from the Lamb shift effect.

## I. INTRODUCTION

THE recent experiments in high-energy electron scattering[1] and mesonic x-rays[2] have indicated that the nuclear charge distribution probably consists of a central region of uniform density with an extended "tail" at the periphery of the latter and with a root-mean-square radius of $R=r_0A^{\frac{1}{3}}$, where $A$ is the atomic mass number and $r_0\cong1.2\times10^{-13}$ cm.[3] Cooper and Henley[4] and Ford and Hill[5] have compared these and other methods yielding information on the nuclear charge distribution and find, with one exception, that the results of the various experiments are consistent with this value of $r_0$.

This exception is the value of $r_0$ obtained by Schawlow and Townes.[6] Using the method of Broch,[7] they have calculated the change in the electronic energy levels due to finite nuclear size. A correction term for the $2p_{\frac{1}{2}}-2p_{\frac{3}{2}}$ ($L_{II}$–$L_{III}$) fine structure splitting was evaluated and added to the splitting formula of Christy and Keller[8] which had been derived by assuming a point nucleus. A comparison of the theoretical fine structure splitting (without the nuclear size correction) with measured values obtained from the tables of Cauchois and Hulubei[9] showed a systematic deviation for large atomic number which had a direction and order of magnitude predicted by the nuclear size effect theory. Under the assumption that the deviation was due entirely to the finite nuclear size, Schawlow and

* Work supported by the U. S. Atomic Energy Commission.
† Based on a Ph.D. thesis submitted by R. L. Shacklett, California Institute of Technology, 1956 (unpublished).
‡ Present address: Department of Physics, Fresno State College, Fresno, California.
[1] Hofstadter, Hahn, Knudsen, and McIntyre, Phys. Rev. **95**, 512 (1954).
[2] V. L. Fitch and J. Rainwater, Phys. Rev. **92**, 789 (1953).
[3] Hill, Freeman, and Ford, Phys. Rev. **99**, 649(A) (1955).
[4] L. N. Cooper and E. M. Henley, Phys. Rev. **92**, 801 (1953).
[5] K. W. Ford and D. L. Hill, Phys. Rev. **94**, 1630 (1954).
[6] A. L. Schawlow and C. H. Townes, Phys. Rev. **100**, 1273 (1955). We wish to thank the authors of this paper for providing us with a copy of the unpublished manuscript which formed a basis for planning portions of the present measurements.
[7] E. K. Broch, Arch. Math. Naturvindenskab **48**, 25 (1945).
[8] R. F. Christy and J. M. Keller, Phys. Rev. **61**, 147 (1942).
[9] Y. Cauchois and H. Hulubei, *Longueurs d'Onde des Emissions X et des Discontinuities d'Absorption X* (Hermann et Cie, Paris, 1947).

Townes evaluated the nuclear size correction parameter by a least-squares fit of theoretical and experimental values and obtained a value of $r_0=(2.1\pm0.2)\times10^{-13}$ cm.

Inasmuch as the evidence in favor of the smaller value for $r_0$ ($1.2\times10^{-13}$ cm) is now very strong, it has been suggested[5,6,10] that quantum electrodynamic effects such as vacuum polarization and the "Lamb shift" probably modify the fine structure splitting to such an extent that the correction in terms of a fictitious nuclear size requires an unusually large value of $r_0$. The contribution of vacuum polarization to the $L_{II}$–$L_{III}$ x-ray level splitting has been calculated recently by Wichmann and Kroll.[11] It is possible, therefore, to make a correction for this effect and for the effect of a nuclear radius with $r_0=1.2\times10^{-13}$ cm. Any remaining discrepancy between theoretical and measured values of the $L_{II}$–$L_{III}$ splitting could therefore be attributed to Lamb shift effects and possibly small residual errors in the point-nucleus expression of Christy and Keller.

The existing x-ray data used by Schawlow and Townes evidently contain random errors of about 0.05% as indicated by Fig. 5 of their paper. It is clear that an increase in precision of the x-ray measurements by a factor of ten would make possible more definitive conclusions based on the fine structure anomaly. At the suggestion of C. H. Townes, the present investigation was undertaken to improve on the precision of the x-ray data entering into the Schawlow-Townes theory.

The $L_{II}$–$L_{III}$ energy level difference can be measured in several different ways, each having its own set of experimental difficulties. A direct determination of the energies of the two levels can be made by absorption edge measurements. This method is not suitable for high precision work, however, because of the uncertainties in the exact position of the "edge" introduced by solid-state effects. The difference in energies of the two levels can be obtained from several pairs of x-ray lines. The $K\alpha_1-K\alpha_2$ doublet could be used, but the relatively large energy of these lines introduces several complications into an experiment; also the fact that these lines have a rather large energy width compared to $L$-series lines places limitations on their usefulness as a precision measure of the level splitting. Six different pairs of $L$-series lines might be used, but because fluorescent sources were employed intensity considerations were acutely important and hence only the $L\beta_1-L\alpha_2$ pair proved to be suitable for this type of work.

Using two-crystal spectrometer techniques, we have made precision measurements of the Bragg angles of the $L\beta_1$ and $L\alpha_2$ x-ray lines of the six heavy elements W, Pt, Bi, Th, U, and Pu. The values of the $L_{II}$–$L_{III}$ fine structure splitting calculated from these data have an accuracy of about 50 parts per million, roughly ten times the accuracy of previous measurements. A comparison of the transition energies of the lines calculated from the present data with those calculated from the tabulated wavelengths[9] reveals a possible systematic error in the earlier measurements of the $L\alpha_2$ wavelengths for several elements of high $Z$. This error is in such a direction as to yield a value of the fine structure splitting for these elements which is too small. Thus the large value of $r_0$ obtained by Schawlow and Townes may be due partly to this supposed error, since the effect of finite nuclear size is to decrease the level splitting.

The improved precision of the measurements makes it possible to evaluate an empirical correction term for the Lamb shift effect under the assumption that the point-nucleus expression contains no errors. Work is at present under way by S. Cohen to recalculate the $L_{II}$–$L_{III}$ splitting to higher accuracy than was attained by Christy and Keller.

## II. EXPERIMENTAL

### X-Ray Sources

In view of the fact that commercial, sealed off x-ray tubes with targets of the requisite high atomic numbers are either difficult or impossible to obtain, it was decided to use the fluorescent-type source. It was felt that, for work of the high precision here required, demountable x-ray tube sources would hardly afford the requisite stability of intensity. In any case, plutonium could not have been made available to us for use as an x-ray tube target. In an experiment similar in several respects to the present one, Rogosa and Schwarz[12] found that a fluorescent source gave sufficient intensity for precision measurements, and their success encouraged us to try it.

The six elements studied are all available in the metallic state and hence are easily mounted in the form of a flat strip or plate on an aluminum holder. The holder design is shown in Fig. 1 and has the feature that the fluorescent radiation can be seen both by the spectrometer and by a monitoring Geiger counter positioned off to one side. The holder accommodates flat strips of metal about $\frac{3}{4}$ in.$\times2\frac{1}{2}$ in. The plutonium source,[13] because of its toxic properties, was "sandwiched" between two aluminum protective plates. The top plate was provided with a window, covered with 6-mil aluminum foil, whose opening was the size of the Pu strip.

The exciting radiation was obtained from a Machlett type OEG–50T high-intensity tungsten-target x-ray tube. The tube was positioned over the fluorescer so that the tube window was parallel and as close as practicable to it. X-ray tube power was obtained from a Phillips water-cooled diffraction unit with regulated primary voltage.

[10] C. H. Townes, Phys. Rev. **94**, 773 (1954).
[11] E. H. Wichmann and N. M. Kroll, Phys. Rev. **101**, 843 (1956).
[12] G. L. Rogosa and G. Schwarz, Phys. Rev. **92**, 1434 (1953).
[13] We wish to acknowledge the cooperation of Dr. Eric Jette at the Los Alamos Scientific Laboratories under whose direction this Pu sample was prepared.

As a precaution against errors arising from variations in intensity of the source during measurements on a spectral line, counts from the monitoring Geiger counter were fed into an electromechanical scaler which could be preset to any given total number of counts. The counting time interval was controlled by this scaler so that if the source intensity dropped or rose slightly during measurements at a particular spectrometer setting, the time interval would be lengthened or shortened to compensate for the change in intensity.

The source, x-ray tube, and monitor with its shielding were mounted on a thick steel base plate and enclosed in a lead-lined box. The box was provided with adjustable vertical and horizontal slits immediately in front of the source holder. Pin-hole photographs of the fluorescer indicated that its intensity was essentially uniform in both the horizontal and vertical directions.

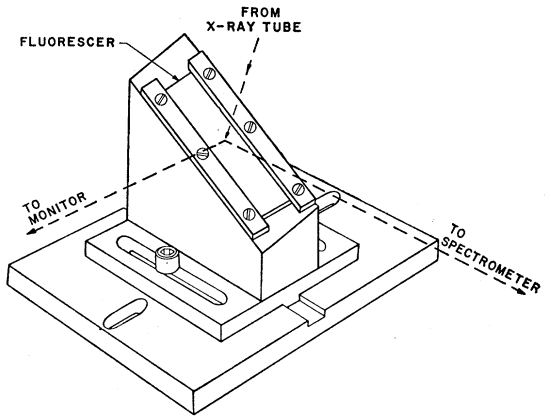


FIG. 1. The fluorescent source holder. The x-ray tube window is positioned just a few cm above the slanting surface so that the exciting radiation is essentially normal to the source plane.

## Spectrometer

The two-crystal spectrometer used in these investigations was designed by one of us and is described in some detail elsewhere.[14] Additional discussion related to the use of the instrument by W. J. West in a precision determination of the wavelength of the W $K\alpha_1$ line may be found in a paper published in 1949.[15] Briefly, the instrument is provided with four independent motions of rotation actuated by worm wheel drives which permit [(a) and (b)] precision settings of the two crystal tables to a few tenths of a second of arc, (c) angular setting of the instrument as a whole about an axis coincident with that of crystal $A$ relative to the primary x-ray beam, and (d) angular setting of the arm supporting the x-ray detector about an axis coincident with that of crystal $B$. The worm gears on which the crystal tables are mounted have been specially lapped and optically calibrated by methods described in an earlier article.[14]

In the present investigation large calcite crystals ($2\frac{3}{4}$ in. on a side, 1 in. thick) were employed whose reflecting surfaces were ground, polished, and etched according to the technique of Manning.[16] The angular widths of the parallel-position rocking curves obtained with these crystals were found to increase approximately linearly with wavelength and with a width at a given wavelength about 2 seconds of arc wider than predicted by the theory for perfect calcite crystals. Hence these crystals probably deviate slightly from perfection because of a residual surface mosaic structure produced by grinding which possibly could have been removed by continued careful polishing and etching. However, it was thought best not to attempt to achieve a slight gain in resolving power with the attendant decrease in luminosity when the usefulness of the crystals in precision wavelength determinations would not be materially improved.

The temperature of the spectrometer and crystals was maintained at a desired value to within about 0.2°C by means of electrical room heaters controlled by a Fenwal Thermoswitch. An aluminum isothermal heat shield was placed over the crystals to prevent air currents from causing temperature changes in the grating constant of that part of the lattice in the reflecting surfaces. Windows in the heat shield covered with $\frac{1}{4}$-mil Mylar allowed passage of the x-ray beam with negligible loss due to absorption.

## Detector

The x-ray detector used in this work was a NaI scintillation crystal mounted in its holder on the face of a DuMont 6292 photomultiplier tube. The detector was fabricated by Robert Swank of the Argonne National Laboratories and consists of a round, thin (about 0.1 in.) wafer of NaI which is mounted in a holder having a beryllium window for the x-rays and a glass window for the light output. The tube and crystal were enclosed inside a brass cylindrical housing provided with a light-tight paper window for the x-rays. On this same housing was mounted the detector slit system consisting of a pair of horizontal and vertical slits defining a rectangular aperture about $\frac{3}{8}$ in. wide by $\frac{1}{2}$ in. high. The slit sizes were changed for different x-ray lines depending on the Bragg angle and the usable height of the source. The whole assembly was mounted on the detector support arm of the spectrometer which also held a preamplifier for the photomultiplier tube output.

Conventional electronics was used in the remainder of the detecting system: a linear amplifier, a pulse-height analyzer, and a scaler. The pulse-height analyzer was used to eliminate background arising from phototube and amplifier noise and from cosmic rays. With no special techniques being used, it was possible to detect

[14] J. W. M. DuMond and D. Marlow, Rev. Sci. Instr. **8**, 112 (1937).
[15] Watson, West, Lind, and DuMond, Phys. Rev. **75**, 505 (1949).
[16] K. V. Manning, Rev. Sci. Instr. **5**, 316 (1934).

TABLE I. Results of Mo $K\alpha_1$ Bragg angle measurements, uncorrected for vertical divergence.

| Run | $180°+2\theta$ | Worm wheel correction $\Delta\theta_w$ | Temperature correction $\Delta\theta_t$ | Bragg angle $\theta$ |
|---|---|---|---|---|
| $L_1$ | 193° 25′ 14.9″ | −4.3″ | 1.6″ | 6° 42′ 36.9″ |
| $R_1$ | 193° 25′ 14.5″ | −4.3″ | 1.7″ | 6° 42′ 36.8″ |
| $R_2$ | 193° 25′ 17.1″ | −5.0″ | 1.6″ | 6° 42′ 37.7″ |
| $L_2$ | 193° 25′ 17.0″ | −5.0″ | 1.7″ | 6° 42′ 37.7″ |
| $L_3$ | 193° 25′ 19.1″ | −8.0″ | 1.7″ | 6° 42′ 37.3″ |

x-rays of energy as low as about 8 kev with a minimum of background.

## Procedure

Inasmuch as the calibration of the two precision worm wheels which drive the crystals had not been checked for several years, it was decided to make a preliminary measurement of the Bragg angle of the Mo $K\alpha_1$ x-ray line. This particular line has been measured by many investigators, and its wavelength is essentially a standard for the x-ray scale. The Bragg angle for calcite has been measured by Compton[17] using two-crystal spectrometer techniques; when the vertical divergence correction of Williams[18] is applied, the resultant Bragg angle as obtained by Compton is

$$\theta = 6° 42' 35.9_5'' \text{ (at 18°C)}. \quad (1)$$

By making measurements of this angle in several different portions of the worm wheel of crystal $B$, the accuracy of calibration could be checked as well as the grating space of the calcite used in the present work.

Using a fluorescent Mo source, five independent sets of measurements of the Bragg angle were made, each measurement consisting in the complete delineation of a parallel $(1, -1)$ and antiparallel $(1,1)$ curve. The angular displacement between the centers of the two curves is equal to $180°+2\theta$, where $\theta$ is the Bragg angle uncorrected for worm-wheel errors, vertical divergence, and temperature. In some of the measurements the beam was deviated to the left by crystal $A$, and in others to the right. We shall denote runs of the former type by the letter $L$ and runs of the latter type by the letter $R$. Subscripts appended to these letters distinguish the three different portions of the worm wheel of crystal $B$ that were used.

The results of the preliminary measurements on Mo $K\alpha_1$ are shown in Table I. The worm-wheel readings required correction for worm-wheel errors. These were taken from the calibration curves which had been prepared by optical tests when the instrument was first constructed.[14] The worm-wheel correction, $\Delta\theta_w$, is equal to the difference between the parallel position correction and the antiparallel position correction; the sign is determined by whether the antiparallel angle is subtracted from the parallel angle to determine $180°+2\theta$ or vice versa. The correction $\Delta\theta_w$ is added to $180°+2\theta$ while the temperature correction,[17] $\Delta\theta_t$, is added to $\theta$. The vertical divergence correction is the same for all runs and amounts to 1.4 seconds as computed from Williams' formula[18]:

$$\Delta\theta_v = \left(\frac{h_1^2+h_2^2}{24L^2}\right)\tan\theta, \quad (2)$$

where $h_1$ and $h_2$ are the heights of the two slits limiting the angle of vertical divergence of the beam and $L$ is the distance between them. The mean value of the five measurements with its standard deviation is

$$\theta = 6° 42' 35.9 \pm 0.2''.$$

The remarkable agreement between this and Compton's value of $\theta$ [Eq. (1)] may be somewhat fortuitous, but it indicates that the crystals, worm-wheel calibration, and techniques do not give rise to large systematic errors and are probably reliable for precision wavelength measurements.

In the case of the $L$-line investigations, four independent determinations of the Bragg angles of the $L\beta_1$ and $L\alpha_2$ lines were made for each of the six elements by using two different regions of the crystal $B$ worm wheel. Measurements were made in the usual way by advancing the spectrometer one or two seconds of arc at a time over the parallel curve and five or ten seconds at a time over the antiparallel curve. At each setting, the x-ray intensity would be determined by accumulating counts over a sufficient time interval to obtain good counting statistics. The time interval, of course, was essentially the same[19] for all the points on a given curve.

For all the $L\alpha_2$ lines and for the Pu $L\beta_1$ line, the intensity was too low to get the desired number of counts at the peak (about 8000) in just one run over the line. Therefore two and sometimes three runs were necessary in order to make the time per run of reasonable length. For example, a total of twelve hours were required for the three runs over the Pu $L\alpha_2$ line. The temperature was maintained at a constant value to within one or two tenths of a degree during the course of a series of runs. In the parallel position, the intensity was high enough so that the x-ray tube could be run at reduced power. Under these conditions the tube current was stable enough so that the use of the monitor to compensate for intensity variations was not warranted. The counting time interval was controlled by the 60-cycle power-line frequency instead.

## III. CORRECTIONS

In attempting to compensate partly for the low intensity of a fluorescent source by using as broad a source as possible, the disturbing effects of large vertical

[17] A. H. Compton, Rev. Sci. Instr. **2**, 365 (1931).
[18] J. H. Williams, Phys. Rev. **40**, 636 (1932).
[19] The time interval, being controlled by the monitor scaler, would be subject to slight variations from point to point because of possible variations in x-ray intensity and monitor counting statistics. The time was recorded for each point and the counting data normalized to counts per unit time.

divergence are introduced. These effects are the broadening and distorting of a spectral line and the shift of the center of the line to longer wavelengths. In this section we shall describe the analysis of this aberration and the methods used to correct for it. We shall also discuss a correction for a less significant effect, namely, the shift in the center of the line due to the well-known crystal diffraction pattern asymmetry first predicted in Darwin's dynamical theory.[20] The shifting effect of absorption in the source and air path on the position of a spectral line (because of the slight variation in absorption coefficient across the line profile) was also analyzed but was found to be negligible and will not be discussed further.

### Vertical Divergence

In what follows we shall refer frequently to "the center point of a spectral line profile." By this we shall mean the center of a horizontal chord drawn across the line at half maximum height.

The problem of the correction for the displacement of the center of a spectral line due to vertical divergence has been investigated by others. Williams[18] and Spencer[21] give correction formulas for the effect; Spencer's formulas are based on the assumption that the center of the spectral line will be shifted the same amount as the center of gravity of the "geometrical window curve"[22] of the spectrometer. Allison[23] has shown the effect of vertical divergence on a hypothetical "monochromatic" spectral line by numerical evaluation and integration of the two-crystal Prins diffraction pattern.

Under the normal requirements of precision in x-ray spectroscopy, it is usually sufficient to draw a smooth curve through the observed points on the spectral line, locate the midpoint (usually at half-maximum intensity), and correct the results for vertical divergence by using the appropriate formula. It was believed, however, that the data obtained in the present work required a more refined treatment inasmuch as the desired precision was somewhat greater. The plan was to fit the observed points to a theoretical curve which would take into account not only the shift in wavelength of the observed spectral line but also its broadening and distortion as well. The analytical fitting of the data to a theoretical spectral line profile makes it possible to use the data more efficiently, an important consideration when intensity is at a premium.

Our derivation of the theoretical line shape as modified by the two-crystal spectrometer with finite vertical divergence is based primarily on three assumptions. (1) The original spectral line (as emitted by the source) is assumed to have the shape of a witch.[24] (2) The two-crystal Prins diffraction pattern under conditions of zero vertical divergence is also assumed to be sufficiently well approximated for our purpose by the shape of a witch. (3) It is assumed that the spectral line shape which the spectrometer would give for nonzero vertical divergence is the fold of the geometrical window curve and the spectrometer line shape for zero vertical divergence.

Assumption (1) is well justified both in theory and experiment.[25] The main justification for (2) is that it greatly simplifies the calculations. Actual comparison of Allison's monochromatic two-crystal diffraction pattern[23] with a witch having the same amplitude and half-width (for the case of calcite at 1.537 A) indicates that although the witch is slightly wider at the base than Allison's curve the disagreement is not serious enough to invalidate the assumption. The simplification lies in the fact that a fold of two witches is itself a witch whose half-width is the sum of the half-widths of the two original witches. Assumption (3) is based on the fact that since the effects of vertical divergence are known to be small, the geometrical window can be separated from the true diffraction pattern without introducing appreciable error.

The two-crystal spectrometer geometrical window curve for point and uniform sources has been discussed elsewhere.[21,26] For the case of the uniform source the curve may be represented by the function

$$G(\lambda')=[2\lambda(\lambda-\lambda')]^{-\frac{1}{2}}-(\lambda\phi_m)^{-1},$$
$$G(\lambda')=0, \quad \lambda'<\lambda_m; \quad \lambda'>\lambda. \tag{3}$$

Here $\lambda$ is the antiparallel spectrometer setting corresponding to the Bragg equation $\lambda=2d_1\sin\theta$, $\theta$ being the Bragg angle made by a ray with zero vertical divergence angle. The angle of *maximum* divergence, $\phi_m$, is related to $\lambda_m$, the *minimum* wavelength that is transmitted through the system, by the equation

$$\lambda_m=\tfrac{1}{2}\lambda(1-\phi_m^2). \tag{4}$$

[20] C. G. Darwin, Phil. Mag. **24**, 325, 675 (1914). See also A. H. Compton and S. K. Allison, *X-Rays in Theory and Experiment* (D. Van Nostrand Company, Inc., New York, 1935), pp. 376–399.

[21] R. C. Spencer, Phys. Rev. **38**, 618 (1931).

[22] We here use the term "geometrical window curve" in the same limited sense as the term "geometrical rocking curve" used by Compton and Allison in their text (reference 20, pp. 735–737). In this sense the geometrical window curve of the two-crystal spectrometer describes the finite spectral intensity distribution which, at a fixed crystal setting, the combination of two successive crystal reflections would select solely because of the finite vertical divergence or "cross fire" of the x-rays, all other effects tending to impair the resolution being excluded. The shape of this geometrical window curve depends therefore on the distribution of x-ray intensity over the various directions of vertical divergence and is hence dependent on slit geometry and on the geometrical distribution of intensity as emitted by the extended source. A more complete discussion of this and related matters has been given in the thesis of one of the authors, R. L. Shacklett, California Institute of Technology, 1956 (unpublished).

[23] S. K. Allison, Phys. Rev. **44**, 63 (1933).

[24] The witch (sometimes known as the Cauchy distribution) has the formula $y=A(1+x^2/a^2)^{-1}$, with $a$ being the half-width at half-maximum.

[25] A. Hoyt, Phys. Rev. **40**, 477 (1932); G. Brogren, Arkiv Fysik **8**, 391 (1954).

[26] J. W. M. DuMond and A. Hoyt, Phys. Rev. **36**, 1702 (1930); M. Schwarzchild, Phys. Rev. **32**, 162 (1928).

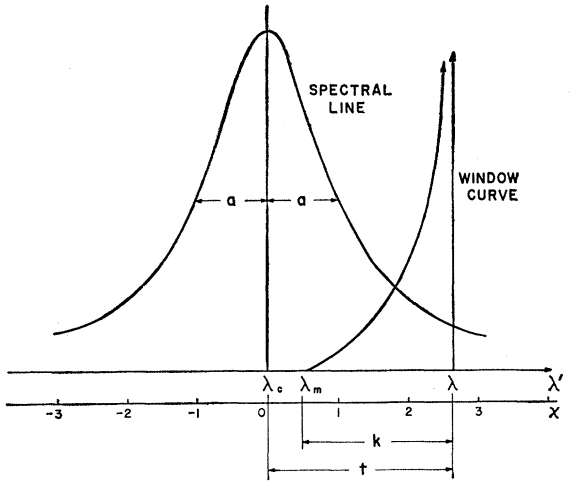


FIG. 2. Curves representing the shape of the spectral line (under the condition of zero vertical divergence) and the geometrical window curve. The spectrometer is set at a wavelength λ corresponding to the Bragg angle θ. The lower scale illustrates the significance of the dimensionless quantities $x$, $t$, and $k$.

Figure 2 shows the geometrical window curve along with the spectral line profile which would be observed under the conditions of zero vertical divergence. We shall let this profile be represented by the function

$$J(\lambda-\lambda_c)=C[1+(\lambda-\lambda_c)^2/a^2]^{-1}, \tag{5}$$

where $\lambda_c$ is the wavelength of the axis of symmetry of this "unmodified line."

The spectrometer output curve (the "modified line") is given by

$$F(\lambda,\lambda_m)=\int_{\lambda_m}^{\lambda} G(\lambda')J(\lambda'-\lambda_c)d\lambda'. \tag{6}$$

We shall make the substitutions

$$x=(\lambda'-\lambda_c)/a, \quad t=(\lambda-\lambda_c)/a, \quad k=(\lambda-\lambda_m)a\cong\lambda_c\phi_m^2/2a, \tag{7}$$

which reduce (6) to

$$F(t,k)=\tfrac{1}{2}C\phi_m k^{-\frac{1}{2}}\int_{t-k}^{t}(t-x)^{-\frac{1}{2}}(1+x^2)^{-1}dx - \tfrac{1}{2}C\phi_m k^{-1}\int_{t-k}^{t}(1+x^2)^{-1}dx. \tag{8}$$

The physical interpretation of the quantities $x$, $t$, and $k$ follows easily from (7). The half-width $a$ of the unmodified line is chosen as a unit of wavelength, and deviations from the wavelength of the center of the unmodified line are measured in terms of this unit. The variable $t$ represents the spectrometer setting, with $t=0$ corresponding to the center of the unmodified line. The parameter $k$ is the wavelength width of the geometrical window in units of $a$. Figure 2 illustrates the relation between these various quantities.

The evaluation of the integrals in (8) is straightforward, but the resulting expression is rather complex and not very illuminating. In order to obtain quantitative information from the results, it was necessary to plot curves of $F(t,k)$ for several values of $k$. The evaluation of the function for values of $t$ in the range $-5<t<5$ and for eleven values of $k$ up to $k=1.5$ was done by electronic computer techniques.[27] Large scale graphs were plotted and measurements were made of the half-width at half-maximum and the shift of the center at half maximum. Figure 3 serves to define these two quantities, $\tau$ and $\delta$. The unmodified line is also shown in the figure so that the effect of vertical divergence is clearly seen.

Graphs of $100(\tau-1)$ and $\delta$ as functions of $k$ are shown in Fig. 4. The quantity $100(\tau-1)$ is the percent increase in half-width of the curve since the half-width of the original curve is unity. An attempt was made to find a simple analytic expression for $\tau$ as a function of $k$, but it was without success. The $\delta$ graph may be expressed quite accurately, however, by the equation $\delta=k/6$. The corresponding shift in wavelength is $ka/6$, and when this is combined with the differential of the Bragg law we obtained a correction formula for the angle to be subtracted from the observed Bragg angle to correct for vertical divergence:

$$\Delta\theta_v=(1/6\lambda_c)ka\tan\theta=(1/12)\phi_m^2\tan\theta. \tag{9}$$

This result agrees with Williams' formula (2) when the slit heights are the same.

The eleven graphs of $F(t,k)$, besides providing information on wavelength shift and increase in width of the modified line, formed a basis for evaluating $F(t,k)$ for any value of $k$ not equal to one of the original 11 values. It can easily be shown that

$$\Delta F=\{\tfrac{1}{2}k^{-1}\tan^{-1}k[t(t-k)+1]^{-1}-\tfrac{1}{2}F(t,k)\}\Delta k/k. \tag{10}$$

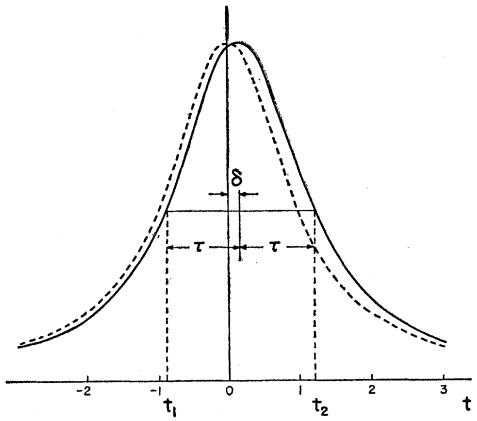


FIG. 3. Plot of $F(t,k)$ for $k=1.0$ showing the significance of $\tau$ and $\delta$. The unmodified witch is shown by the dashed curve.

[27] The machine evaluation of $F(t,k)$ was done by T. W. Layton on a Datatron computer.

The computer program was arranged to compute the quantity in brackets and print out its value along with $F(t,k)$. In this way the experimental data could be fitted to a theoretical curve having a $k$ value slightly different from one of the original values without having to recompute $F$ by machine.

The value of $k$ for a given spectral line depends on the half-width, $a$, of the unmodified line which is actually an unobservable quantity. An excellent approximation for $k(=k')$ may be obtained, however, by using the observed half-width $a'$ and calculating a trial value of $k'$ from (7). This value of $k'$ is then increased by the percentage shown in the first graph of Fig. 4, i.e.,

$$k \cong k' + (\tau - 1)k' = k'\tau. \tag{11}$$

### Crystal Diffraction Pattern Asymmetry

Allison's[23] work on the evaluation of the two-crystal Prins diffraction pattern with and without vertical divergence shows clearly that the asymmetry in the single-crystal diffraction pattern (predicted by the "dynamical theory" with non-negligible absorption) results in a slight shift of the center of a spectral line toward smaller Bragg angles. We are here assuming that this shift is the only aberration and that any other distortions or asymmetries in the "unmodified line"[28] are negligible.

Because of the complexity of the Prins single-crystal diffraction pattern formula, it is impractical to determine an analytic expression giving the shift of the two-crystal diffraction pattern. If the function is graphed, however, it is possible to obtain a sufficiently accurate measure of the shift. Since the absorption in the crystal is a function of wavelength, the asymmetry being more pronounced for the longer wavelengths, the shift would be expected to increase with $\lambda$ in some regular manner. Allison's curve was evaluated for $\lambda = 1.537$ A, and Parratt[29] has published numerical tables for the single-crystal diffraction pattern at $\lambda = 2.299$ A from which it is possible to get the two-crystal diffraction pattern by numerical integration.

Measurements made on the 1.537 A curve show that the shift (which we shall designate by the letter $\epsilon$), when measured in units of rotation of crystal $B$, is about 0.5 sec. At $\lambda = 2.299$ A, $\epsilon = 1.1$ sec. These two values, plus the fact that $\epsilon = 0$ for $\lambda = 0$, make it possible to evaluate an empirical correction formula for this effect. Assuming a power law dependence, we obtain the approximate result

$$\epsilon \cong 0.2\lambda^2 \text{ seconds} \quad (\lambda \text{ in A}). \tag{12}$$

Since $\epsilon$ is measured in terms of the rotation of crystal $B$, the actual correction to be added to the Bragg angle is $\epsilon/2$ inasmuch as the dispersion of the instrument is twice that given by the differential of the Bragg law. The size of the correction varies from about 0.25 second for W $L\alpha_2$ to about 0.05 second for Pu $L\beta_1$. For the purposes of the present work it is more important to know accurately the *differences* between the various corrections applied to the $L\alpha_2$ and $L\beta_1$ angle measurements rather than to know the absolute value of a given correction with high accuracy.

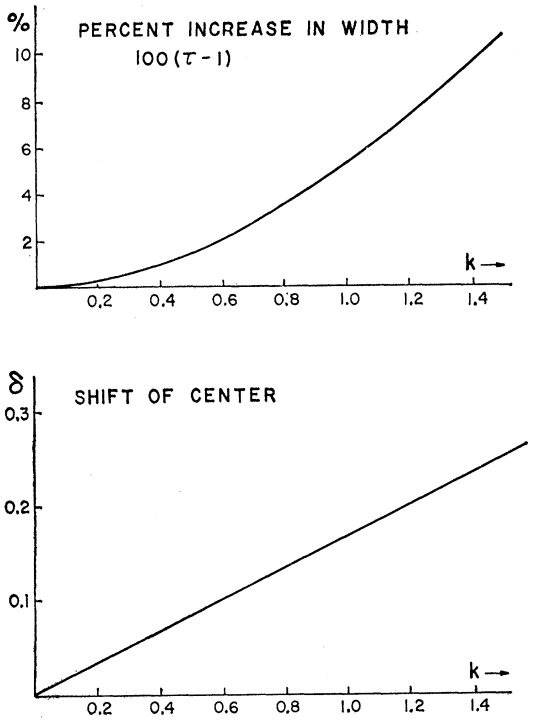


FIG. 4. Curves showing the quantities $100(\tau-1)$ and $\delta$ as functions of $k$.

## IV. RESULTS

The raw data from the various antiparallel runs were subjected to two minor corrections before being fitted to the theoretical line profile $F(t,k)$. The natural background count was subtracted off and also any further background due to any extraneous x-ray lines in the vicinity. This latter correction was made by assuming that the unwanted line had the shape of a witch and subtracting off the intensity due to it in the region of the desired line.

In fitting the data to the theoretical profile, a $k$-value was first determined from the known vertical divergence angle, $\phi_m$, and the half-width of the modified line. A graph of $F(t,k)$ was then drawn to a large scale and the height and half-width determined. The observed data were then normalized to the same height and width as $F(t,k)$. An arbitrary origin, $t'=0$, was established near the center of the observed line profile, and the various spectrometer settings were measured from this origin in half-width units. The intensity at

[28] By the term "unmodified line" we mean the spectral line shape which the spectrometer would give for vanishingly small vertical divergence.

[29] L. G. Parratt, Phys. Rev. 41, 561 (1932).

TABLE II. Typical Bragg angle calculations for Bi $L\alpha_2$ and Bi $L\beta_1$ lines.

| Run | Parallel position | Antiparallel position | Worm-wheel correction $\Delta\theta_w$ | $2\theta$ (uncorrected) | $\Delta\theta_t+\epsilon/2$ | $\theta$ (corrected Bragg angle) |
|---|---|---|---|---|---|---|
| | | | (a) Bi $L\alpha_2$ runs | | | |
| $L_1$ | 250° 41′ 9.2″ | 48° 44′ 32.6″ | −8.1″ | 21° 56′ 28.5″ | 3.5″+0.1″ | 10° 58′ 17.9″ |
| $R_1$ | 48° 44′ 16.3″ | 250° 40′ 53.8″ | −8.1″ | 21° 56′ 29.4″ | 3.6″+0.1″ | 10° 58′ 18.4″ |
| $L_2$ | 296° 37′ 42.5″ | 94° 41′ 8.2″ | −5.4″ | 21° 56′ 28.9″ | 4.0″+0.1″ | 10° 58′ 18.5″ |
| $R_2$ | 94° 40′ 43.5″ | 296° 37′ 16.4″ | −5.4″ | 21° 56′ 27.5″ | 4.1″+0.1″ | 10° 58′ 18.0″ |
| | | Mean value of Bragg angle for Bi $L\alpha_2$: $\theta=10°\ 58'\ 18.2\pm0.2''$ | | | | |
| | | | (b) Bi $L\beta_1$ runs | | | |
| $L_1$ | 248° 44′ 11.3″ | 50° 41′ 28.4″ | −8.6″ | 18° 2′ 34.3″ | 2.9″+0.1″ | 9° 1′ 20.2″ |
| $R_1$ | 50° 41′ 9.2″ | 248° 43′ 53.0″ | −8.6″ | 18° 2′ 35.2″ | 2.9″+0.1″ | 9° 1′ 20.6″ |
| $L_2$ | 294° 40′ 47.2″ | 96° 38′ 6.6″ | −6.3″ | 18° 2′ 34.3″ | 3.2″+0.1″ | 9° 1′ 20.5″ |
| $R_2$ | 96° 37′ 39.9″ | 294° 40′ 21.7″ | −6.3″ | 18° 2′ 35.5″ | 3.2″+0.1″ | 9° 1′ 21.0″ |
| | | Mean value of Bragg angle for Bi $L\beta_1$: $\theta=9°\ 1'\ 20.6\pm0.2''$ | | | | |

each point, designated as a $y$ value, was used to locate a corresponding $t$ value on the large scale plot of $F(t,k)$. Ordinarily a difference would exist between this value of $t$ and the value of $t'$ for the observed point. The size of the difference was a measure of how far the arbitrary origin was from the true origin $t=0$. If each of the observed points fitted the theoretical curve exactly, the difference $t'-t$ would have the same value for each point. However, statistical fluctuations and errors in spectrometer setting cause a variation of the $t'-t$ value from one point to the next. If one assumes random variations, the weighted average of the $t'-t$ value for each point would indicate the spectrometer setting corresponding to the center of the unmodified line. The weight function used was $w=by^2(A-y)$, where $b$ is an arbitrary constant and $A$ is the amplitude of the curve. It was derived assuming the main source of variation in the $t'-t$ values to be the statistical uncertainty in the counts.

These various steps represent a considerable amount of labor for 48 different antiparallel runs. The extra effort is justified, however, since the method gives the center of a line to better than 1/200 of its half-width. A typical graph for Bi $L\beta_1$, run $R_1$, is shown in Fig. 5.

The centers of the parallel rocking curves were much easier to locate because of their narrowness. Instead of

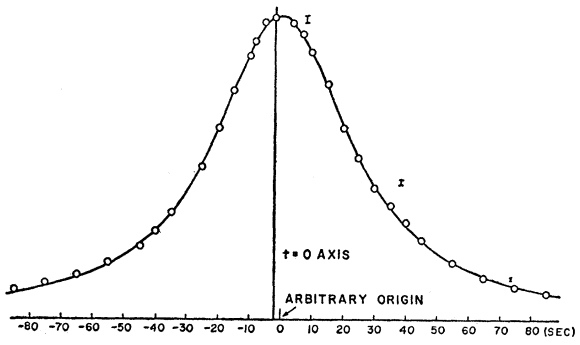


FIG. 5. Typical antiparallel curve (Bi $L\beta_1$; $R_1$) showing the fit of the observed points to the theoretical line profile $F(t,k)$.

drawing a smooth curve through the observed points which were plotted on a large scale, the points were connected by straight line segments. The midpoints of several horizontal lines at different heights drawn from one side of the curve to the other were averaged to give the angle corresponding to the parallel position.

The calculations for the Bragg angle follow from the antiparallel and parallel positions in the same way as for the Mo $K\alpha_1$ case except now there is no explicit vertical divergence correction. Typical angle calculations are shown in Table II for the Bi $L\alpha_2$ and $L\beta_1$ lines. Included in these calculations is the small correction, $\epsilon/2$, for crystal diffraction pattern asymmetry.

The Bragg angles for each of the measured lines are given in Table III with their standard deviations. The wavelengths were calculated from the Bragg law by using the effective first-order grating space, $d_1=3029.04$ $x$ units at 18°C. Values of $\sin\theta$ were independently checked to 8 decimal places by tables and by a power series expansion. The transition energies are given in Rydbergs and in volts with the necessary conversion from $x$ units to milliangstroms made using $\lambda_\theta/\lambda_s=1.002039$, and with $R=109737.309$ cm$^{-1}$, and $E\lambda_s=12372.44$ kev $x$ unit.[30] Shown in Table IV are the values of the fine structure splitting, $\Delta\nu/R$, and their relative errors in parts per million.

A comparison of the present experimental results to the tabulated data[9] used by Schawlow and Townes shows some interesting discrepancies. Figure 6 represents graphically the relative difference in parts per million between the transition energy values computed from the tabulated wavelengths and those listed in Table III. Evidently the differences in the $L\alpha_2$ values for the higher-$Z$ elements are larger than can be accounted for on the basis of random experimental errors, since the $L\beta_1$ differences are reasonably small. The fact that the older $\nu/R$ values for the $L\alpha_2$ lines for Bi, Th, and U are all *larger* than the present values

[30] Cohen, DuMond, Layton, and Rollett, Revs. Modern Phys. **27**, 363 (1955).

TABLE III. Experimental results.

| X-ray line | Bragg angle (calcite) | Wavelength (x units) | Transition energy Rydbergs | Transition energy Electron volts | Relative error[a] (ppm) |
|---|---|---|---|---|---|
| W $L\alpha_2$ | 14° 10′ 59.8±0.3″ | 1484.378±0.008 | 612.656±0.003 | 8335.12±0.05 | 5 |
| W $L\beta_1$ | 12° 11′ 23.9±0.1″ | 1279.186±0.003 | 710.931±0.001 | 9672.14±0.02 | 2 |
| Pt $L\alpha_2$ | 12° 36′ 2.6±0.2″ | 1321.604±0.005 | 688.113±0.003 | 9361.71±0.04 | 4 |
| Pt $L\beta_1$ | 10° 37′ 51.5±0.4″ | 1117.611±0.010 | 813.712±0.008 | 11 070.47±0.10 | 9 |
| Bi $L\alpha_2$ | 10° 58′ 18.2±0.2″ | 1153.001±0.005 | 788.735+0.003 | 10 730.66±0.04 | 4 |
| Bi $L\beta_1$ | 9° 1′ 20.6±0.2″ | 950.031±0.006 | 957.246±0.006 | 13 023.24±0.08 | 6 |
| Th $L\alpha_2$ | 9° 10′ 28.3±0.1″ | 965.914±0.004 | 941.505±0.004 | 12 809.08±0.05 | 4 |
| Th $L\beta_1$ | 7° 14′ 30.2±0.2″ | 763.655±0.005 | 1190.868±0.007 | 16 201.64±0.10 | 6 |
| U $L\alpha_2$ | 8° 44′ 29.0±0.2″ | 920.676±0.006 | 987.767±0.006 | 13 438.47±0.08 | 6 |
| U $L\beta_1$ | 6° 48′ 41.3±0.1″ | 718.505±0.004 | 1265.701±0.007 | 17 219.74±0.10 | 6 |
| Pu $L\alpha_2$ | 8° 20′ 16.2±0.1″ | 878.480±0.002 | 1035.212±0.002 | 14 083.96±0.03 | 2 |
| Pu $L\beta_1$ | 6° 24′ 35.4±0.2″ | 676.321±0.006 | 1344.647±0.011 | 18 293.79±0.15 | 8 |

[a] The relative error is the statistical standard deviation of the experimental measurements.

means that the values of $\Delta\nu/R$ for these elements as used by Schawlow and Townes are *smaller* by several hundred parts per million. It is not too difficult to suggest a possible source of the discrepancy. The $L\alpha_2$ line is just on the long-wavelength side of the intense $L\alpha_1$ line, and unless special precautions were taken it would be rather difficult to assign an accurate wavelength to $L\alpha_2$ because of the tendency of the nonuniform background of the $L\alpha_1$ line to shift the observed peak of $L\alpha_2$ toward shorter wavelength. It is doubtful, however, whether this type of systematic error can account for all the observed discrepancy.

## V. COMPARISON WITH THEORY

The theoretical expression for the $L_{II}$–$L_{III}$ energy level splitting including the Schawlow-Townes correction for the nuclear size effect may be written[31]

$$\left(\frac{\Delta\nu}{R}\right)_{\text{Th}}=\phi(\alpha Z)+BZ^2-\left(\frac{\Delta\nu}{R}\right)_{\text{Exp}}De^{b(Z-60)} \quad (13)$$

where

$$\phi(\alpha Z)=2\alpha^{-2}S(\alpha Z)-2\alpha^2Z^3f(\alpha Z)-2(0.0178)\alpha^4Z^5. \quad (14)$$

The quantity $\phi(\alpha Z)+BZ^2$ is the Christy-Keller[8] expression for the splitting assuming a point nucleus, $\alpha$ being the fine structure constant; $B$ is an undetermined constant. The quantity $D$ appearing in the last term of (13) may be regarded as the nuclear radius parameter; $b$ is a number which depends rather insensitively on the assumed nuclear charge distribution and its radius. The Sommerfeld formula $S(\alpha Z)$ may be calculated with arbitrary accuracy, but $f(\alpha Z)$, representing a first-order correction for electron interactions, must be interpolated from a table in Christy and Kellers' paper. It was found that $\log f(\alpha Z)$, when expressed as a function of $1-(1-\alpha^2Z^2)^{\frac{1}{2}}$, is approximately linear so that Lagrange interpolation is reasonably accurate. The last term in (14) is a small correction which Christy and Keller estimated to make up for the omission of higher order terms in the interaction Hamiltonian used to compute $f(\alpha Z)$.

TABLE IV. Fine structure splitting.

| Element | Rydbergs | Electron volts | Relative error[a] (ppm) |
|---|---|---|---|
| $_{74}$W | 98.275±0.004 | 1337.02±0.05 | 37 |
| $_{78}$Pt | 125.599±0.008 | 1708.76±0.11 | 64 |
| $_{83}$Bi | 168.511±0.007 | 2292.58±0.10 | 42 |
| $_{90}$Th | 249.363±0.009 | 3392.56±0.12 | 34 |
| $_{92}$U | 277.934±0.009 | 3781.27±0.13 | 33 |
| $_{94}$Pu | 309.435±0.011 | 4209.83±0.15 | 36 |

[a] The relative error is the relative standard deviation of the experimental measurements.

[31] See Schawlow and Townes' paper (reference 6) for a discussion of this equation.

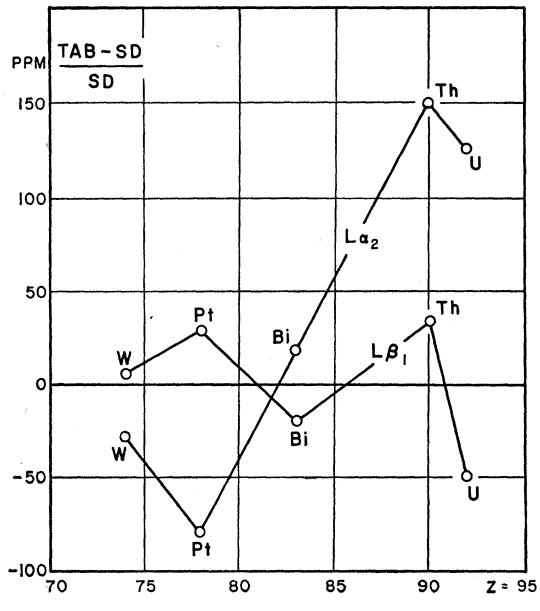


FIG. 6. Graph showing the relative difference between the $\nu/R$ values based on tabulated values of $\lambda$ ("Tab") (reference 9) and those in Table III ("*SD*") for both the $L\alpha_2$ and $L\beta_1$ x-ray lines. The lines between the points are for the purpose of distinguishing one set from the other.

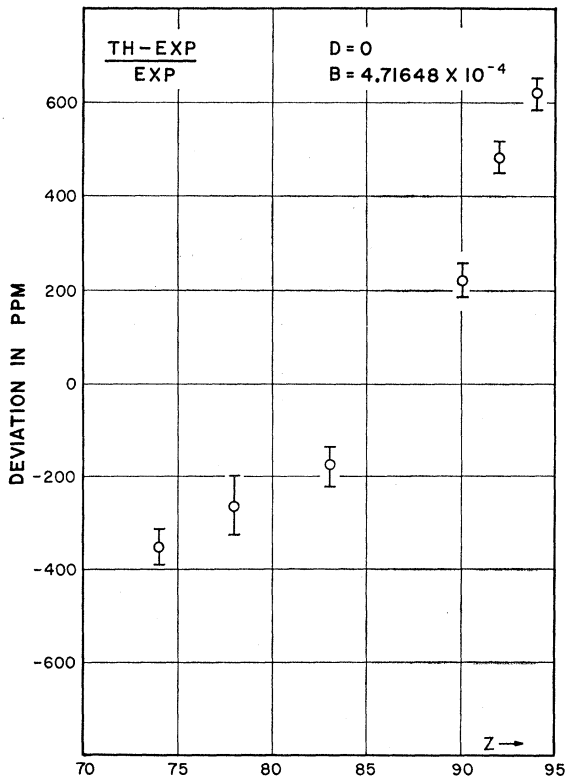


FIG. 7. Relative deviation of theory and experiment without the nuclear size or quantum electrodynamic corrections. The statistical error for the various points is the relative standard deviation of the experimental measurements.

It is necessary to make a correction for the effect of the anomalous electron moment which increases the calculated fine structure by the factor $1+\alpha/\pi$ to first order.[32] To make the comparison between theory and experiment one may apply the correction factor to either quantity; for convenience we shall modify the experimental values of $\Delta\nu/R$ by the factor $(1+\alpha/\pi)^{-1}$.

In making the comparison of theory and experiment we shall proceed in a manner similar to that used by Schawlow and Townes. We shall first assume a point nucleus ($D=0$) and evaluate the constant $B$ in (13) by a least squares fit of the theoretical to the experimental values of $\Delta\nu/R$ [modified by the factor $(1+\alpha/\pi)^{-1}$]. The value of $B$ thus determined is used to calculate the relative deviation between theory (for point nucleus) and experiment as follows:

$$\frac{\text{Th}-\text{Exp}}{\text{Exp}}\equiv\frac{(\Delta\nu)_{\text{Th}}-(\Delta\nu)_{\text{Exp}}}{(\Delta\nu)_{\text{Exp}}}=\frac{Z^2}{\Delta\nu/R}-\left(1-\frac{\phi(\alpha Z)}{\Delta\nu/R}\right). \quad (15)$$

[32] This is the "Bethe-Longmire" correction briefly alluded to by Schawlow and Townes. We wish to acknowledge clarification of this point for us by Professor Townes in private correspondence.

Equal weighting is used in the least squares analysis because the relative errors in the experimental measurements are all about the same (see Table III). In Fig. 7 the results of this first comparison are shown graphically with the relative deviations in ppm plotted against $Z$. The statistical error for the various points is the relative standard deviation of the experimental measurements. It is clear that the improved precision of the x-ray measurements has made the systematic deviation between the point-nucleus theory and experiment at large $Z$ more pronounced than appears in Fig. 5 of Schawlow and Townes' paper. It is to be noted, however, that the magnitude of the deviation for $Z=90$, 92 is significantly smaller in the present comparison.

When the nuclear size effect is included in the theory, two approaches may be followed. We may assume that the deviation between the point nucleus values of $\Delta\nu$ and the experimental values is due entirely to a fictitious uniformly charged spherical nucleus of unknown radius. The values of $D$ and $B$ in (13) may then be adjusted by least squares to give best fit to the experimental data, with the value of $D$ thus obtained being a measure of the nuclear radius. Another approach would be to accept the results of other measurements on nuclear size and charge distribution[1,2] and recompute the value of $D$ and $b$ by extrapolating the Schawlow-Townes calculations which were based on a uniformly charged nucleus of radius $r_0=1.5\times10^{-13}$ cm. This calculation would then permit a comparison of experiment with theory from which the need for further corrections might become apparent.

Ford and Hill[5] have shown that a nuclear charge distribution with an extended tail has a slightly different effect on the x-ray fine structure splitting then that due to a uniformly charged nucleus; little error results, however, from making the simplifying assumption that the charge is uniformly distributed. We shall assume further that the nuclear radius constant $r_0$ has the value $r_0=1.2\times10^{-13}$ cm and correct the Schawlow-Townes results accordingly. We are thus led to the expression

$$\Delta E/h\Delta\nu=De^{b(Z-60)}=0.54\times10^{-4}e^{0.0878(Z-60)}, \quad (16)$$

where $\Delta E$ is the change in fine structure splitting due to this particular nuclear model.

If we now regard the value of $D$ in (13) as unknown and determine it and $B$ by least squares, using the value of $b=0.0878$, we shall be able to find the radius of the fictitious nucleus whose finite extent gives rise to the deviation between theory and experiment shown in Fig. 7. The results of the comparison yield $B=4.81722\times10^{-4}$ and $D=0.44\times10^{-4}$ with a root mean square deviation of 60 parts per million remaining between theory and experiment. This value of $D$ corresponds to a nuclear radius with $r_0=1.08\times10^{-13}$ cm and is to be contrasted with $r_0=2.1\times10^{-13}$ cm obtained by Schawlow and Townes in their comparison using already existing x-ray data. As was pointed out in IV,

a portion of this discrepancy might be attributed to uncertainties in the older wavelength measurements of some of the $L\alpha_2$ lines.

The value of $D$ obtained above ($0.44\times10^{-4}$), when compared with that in (16), suggests that additional correction terms are needed in order to maintain agreement between theory and experiment when a nuclear radius of $r_0=1.2\times10^{-13}$ cm is assumed. One such correction is due to the effect of vacuum polarization. Wichmann and Kroll[11] have made an accurate determination of the contribution of vacuum polarization to the $L_{II}$–$L_{III}$ splitting. They have calculated the contribution in Rydbergs for various values of $Z$ and present the results as $\delta_p^{(1)}$ in Table I of their paper. It was found that the fraction $\delta_p^{(1)}/(\Delta\nu/R)$ could be represented accurately by the formula

$$\delta_p^{(1)}/(\Delta\nu/R)=Ve^{c(Z-60)}, \tag{17}$$

with $V=1.73\times10^{-4}$ and $c=0.0462$. The expression corresponding to (15) which includes both nuclear size and vacuum polarization corrections is

$$\frac{\text{Th}-\text{Exp}}{\text{Exp}}=B\left(\frac{Z^2}{(\Delta\nu/R)}\right)-\left(1-\frac{\phi(\alpha Z)}{(\Delta\nu/R)}\right)$$
$$-De^{b(Z-60)}+Ve^{c(Z-60)}. \tag{18}$$

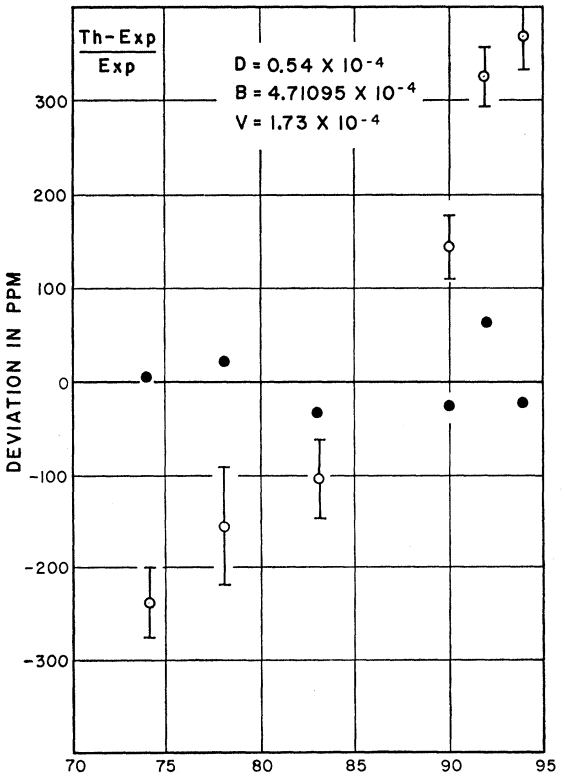


FIG. 8. Relative deviation of theory and experiment when corrections for vacuum polarization and a nuclear radius of $r_0=1.2\times10^{-13}$ cm are included. The statistical error for the various points is the relative standard deviation of the experimental measurements. The solid circles show the effect of the addition of the empirical correction term.

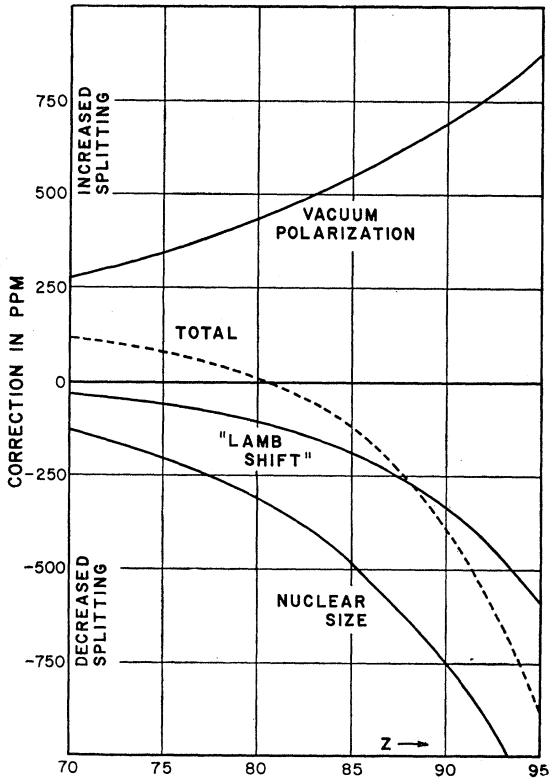


FIG. 9. The effect of the various correction terms on the fine structure splitting as given by the Christy-Keller point-nucleus formula.

With $D$ fixed at $0.54\times10^{-4}$ ($r_0=1.2\times10^{-13}$ cm) and $B$ adjusted by least squares, the resulting relative deviations (the points with open circles in Fig. 8) show that still further corrections are needed in the theory.

It is generally known that the quantum electrodynamic effect commonly referred to as the "Lamb shift" plays an important role in modifying the calculated fine structure splitting. Quantitative evaluations of the correction for $\alpha Z\approx1$ are very difficult and have not been accomplished as yet. It is therefore of some interest to determine from the remaining discrepancy between theory and experiment shown in Fig. 8 the magnitude and $Z$ dependence of the correction required to minimize the discrepancy. Whether or not the correction term thus obtained actually represents the Lamb shift depends on the accuracy of the other quantities entering into the theory. Probably the least precise is the electron interaction correction term $f(\alpha Z)$. However, the $Z$ dependence of the quantum electrodynamic effects is more than likely strong enough to override uncertainties in the magnitude of $\phi(\alpha Z)$.

We shall assume that the required correction term is exponential in $Z$, having the form $Le^{a(Z-60)}$ where both $L$ and $a$ are to be determined by least squares. No doubt other functional forms might be used with similar $Z$ dependence, but the one suggested is probably adequate for the present purpose. The appropriateness of

the choice of function can be tested by a comparison of the resulting rms deviation between theory and experiment to the size of the experimental errors.

We may therefore write

$$\frac{\text{Th}-\text{Exp}}{\text{Exp}}=B\left(\frac{Z^2}{\Delta\nu/R}\right)-\left(1-\frac{\phi(\alpha Z)}{\Delta\nu/R}\right)$$
$$-De^{b(Z-60)}+Ve^{c(Z-60)}-Le^{a(Z-60)}, \quad (19)$$

and adjust $B$, $L$, and $a$ by least squares. The results are $B=4.76450\times10^{-4}$, $L=10.9\times10^{-6}$, and $a=0.115$. When these values are resubstituted in (19) and the rms deviation calculated, the result is 33 ppm which is to be compared to the average experimental error of 41 ppm. The points (solid circles) are plotted in Fig. 8 so that the effect of the correction term may clearly be seen. It may be concluded, therefore, that the assumption of a single correction term of exponential form is adequate in view of the present experimental accuracy.

The three corrections to the fine structure splitting, nuclear size, vacuum polarization, and the empirical "Lamb shift," are shown in Fig. 9 with their sum. The empirical term is in qualitative agreement with the preliminary estimates of Wichmann[33] who suggests that the Lamb shift correction is of opposite sign to vacuum polarization and of about the same magnitude. When the uncertainties in the theory are eventually removed or reduced, this method might prove to be of some value in obtaining an accurate value for $\alpha$, the fine structure constant, using the techniques of Christy and Keller.

## VI. ACKNOWLEDGMENTS

The assistance in the early phases of this experiment of Phillip Miller and Han-Ying Ku is gratefully acknowledged. Mr. John J. Merrill's extensive help both in the measurements themselves and also in the reduction of data was of utmost value. We are also grateful for several profitable discussions with Professor Robert Christy.

[33] E. H. Wichmann (private communication).